PACS numbers: 42.55.Wd; 42.79.Bh
DOI: 10.1070/QE2005v035n11ABEH009791

Compact prisms for polarisation splitting of fibre laser beams

B.L. Davydov, D.I. Yagodkin

Abstract. **Simple compact monoprisms for spatial splitting of polarised laser beams with relatively small diameters (no more than 1 mm) are considered. Prisms can be made of optically inactive $CaCO_3$, α-BaB_2O_4 (α-BBO), $LiIO_3$, $LiNbO_3$, YVO_4, and TiO_2 crystals known in polarisation optics. The exact solution of the Snell equation for the extraordinary wave reflected from a surface arbitrarily tilted to its wave vector is obtained. The analysis of variants of the solution allows the fabrication of prisms with any deviation angles of the extraordinary wave by preserving the propagation direction of the ordinary wave. Three variants of prisms are considered: with minimised dimensions, with the Brewster output of the extraordinary beam, and with the deviation of the extraordinary wave by 90°. Calcite prisms with the deviation angles for the extraordinary beam $\sim 19°$ and 90° are tested experimentally.**

Keywords: *polarisation crystal beamsplitters, polarisation prisms.*

1. Introduction

Fibre and crystal polarisation beamsplitters are inherent elements of laser fibre technology, which is being recently rapidly developed. A typical example of crystal beamsplitters is Glan prisms with air gaps. Crystal beamsplitters are broadband, they split beams by considerable angles and can be used with beams of large cross sections. However, they are quite expensive. In fibre laser technologies, collimated beams of diameter 0.3 – 1 mm are used, as a rule, and therefore there is no point in employing large classical polarisation prisms in such lasers.

In this paper, we describe polarisation prisms intended for operation with collimated beams of small diameter.

2. Monoprisms made of uniaxial crystals based on the total internal reflection of the extraordinary wave

The idea of using the total internal reflection (TIR) of extraordinary waves from the side surface of a crystal prism to increase the splitting angle of polarised beams was proposed in Refs [1] and [2]. In this paper, this idea is realised in calculations of prism beamsplitters made of known optically inactive uniaxial crystals with the average values of the birefringence modulus $|n_o - n_e| \gtrsim 0.1$.

Figure 1 shows the section of a rectangular prism parallel to its bases. Below, we also consider rectangular prisms with oblique-angled bases. For brevity, we will denote the working faces by the boundaries of sections of a rectangular prism by a plane parallel to bases. One can see from Fig. 1 how a simplest prism made of a uniaxial crystal in the form of a parallelepiped with three polished faces (two end and one side faces) splits a nonpolarised beam into two orthogonally polarised beams. The two possible orientations of the optical axis of the crystal lying in the figure plane are denoted by straight lines with two arrows and signs '+' and '−' corresponding to the positive and negative crystals. The size of the square cross section of the prism corresponds to the diameter d of the input collimated beam, so that the latter almost fills the prism. The nonpolarised beam incident on the AD face of the prism splits into the two orthogonally polarised ordinary (o) and extraordinary (e) waves. The beam and ray vectors of the o-wave are directed along the geometric axis of the prism (dot-and-dash line), so that the o-beam comes outside through the BC face without changing its direction. On the contrary, the ray vector of the e-wave makes the angle δ_{1dr} with the geometric axis of the prism. We will call this angle the angle of the first energy drift. In this case, the wave

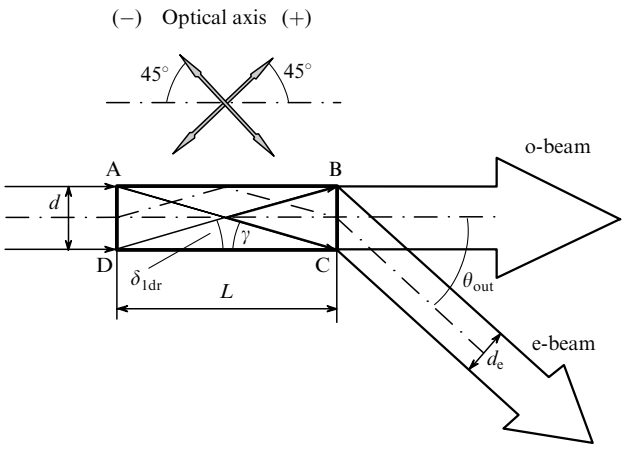

Figure 1. Propagation of beams in a prism polarisation beamsplitter with the reflection of the e-ray from the polished side face.

B.L. Davydov, D.I. Yagodkin Institute of Radio Engineering and Electronics, Russian Academy of Sciences, pl. akad. Vvedenskogo 1, 141120 Fryazino, Moscow region, Russia;
e-mail: bld_res2001@pochta.ru, ydimon@mail.ru

Received 8 June 2005; revision received 7 September 2005
Kvantovaya Elektronika **35** (11) 1064 – 1070 (2005)
Translated by M.N. Sapozhnikov

vector of the e-wave remains parallel to the wave vector of the o-wave. For these orientations of the optical axis, the e-wave experiences TIR from the crystal AB face with the angle of reflection smaller than the 90° angle of incidence. The e-wave comes out to air through the BC face, by refracting at the angle θ_{out}, which is individual for each crystal.

The advantages of such a prism are the simplicity of its design along with rather large beam splitting angles (from 9° to 38°, depending on the crystal type and radiation wavelength, see Table 1 below), the maximum utilisation of the prism volume along with the minimum prism size and the absence of gaps increasing reflection losses or glue connections decreasing the radiation resistance of the device.

The orientation angles of optical axes were chosen to be ±45°, which is close but not equal to the angle of maximum energy drift of extraordinary beams (the difference of these angles from the optimal angle is ±3°). This was done not to unify the orientation of axes upon using different crystals but to minimise the effect of temperature distortions of prisms made of crystals with the anisotropic expansion coefficients. In the case of such an orientation of optical axes, the prism form does not change with temperature. The decrease in the drift angles at the orientation angles ±45° is so small (tenths of degree) that it can be neglected.

The angular characteristics of the polariser shown in Fig. 1 can be calculated from the Snell equation for the e-wave reflected from the side face. This equation was solved by the approximate numerical method [2], which is not very convenient for practical calculations. Our analysis has shown that this equation has the exact solution. Consider now Fig. 2 in which TIR of the e-wave from the AB side surface with the normal N_{AB} tilted to the wave vector $\boldsymbol{K}_{e1}$ of the wave is shown in detail. The extraordinary wave incident on this surface at an arbitrary angle α is reflected from it so that its new wave vector $\boldsymbol{K}_{e2}$ makes the angle $\psi \neq \alpha$ with the normal N_{AB}. When the optical axis lies in the plane of incidence, the Snell equation for reflection has the form

$$\frac{n_o n_e \sin\alpha}{[n_o^2 \sin^2(v-\beta+\alpha) + n_e^2 \cos^2(v-\beta+\alpha)]^{0.5}} =$$

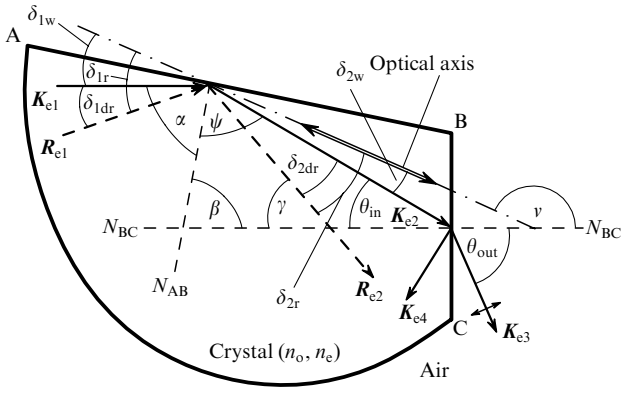

Figure 2. Reflection of waves and rays in a negative uniaxial crystal. $\boldsymbol{K}_{e1}$ and $\boldsymbol{R}_{e1}$: the wave and ray vectors of the incident wave (the AB surface); $\boldsymbol{K}_{e2}$ and $\boldsymbol{R}_{e2}$: the wave and ray vectors of the reflected wave (the AB surface); $\boldsymbol{K}_{e3}$ and $\boldsymbol{K}_{e4}$: the wave vectors of the refracted and reflected waves (the BC surface); $\boldsymbol{N}_{AB}$ и $\boldsymbol{N}_{BC}$: normals to the AB and BC faces.

$$= \frac{n_o n_e \sin\psi}{[n_o^2 \sin^2(v-\beta-\psi) + n_e^2 \cos^2(v-\beta-\psi)]^{0.5}}. \quad (1)$$

The quantities n_o, n_e, α, β, and v in this equation are specified parameters. It is useful to introduce the notation

$$n_\alpha = \frac{n_o n_e}{[n_o^2 \sin^2(v-\beta+\alpha) + n_e^2 \cos^2(v-\beta+\alpha)]^{0.5}}, \quad (2)$$

where n_α is the effective refractive index of the e-wave before its reflection,

$$x_1 = (n_\alpha \sin\alpha)^2 \left[\frac{1}{n_e^2}\sin^2(v-\beta) + \frac{1}{n_o^2}\cos^2(v-\beta)\right], \quad (3)$$

$$x_2 = (n_\alpha \sin\alpha)^2 \left[\frac{1}{n_o^2}\sin^2(v-\beta) + \frac{1}{n_e^2}\cos^2(v-\beta)\right], \quad (4)$$

$$x_3 = (n_\alpha \sin\alpha)^2 \left(\frac{1}{n_o^2} - \frac{1}{n_e^2}\right)\sin(2v-2\beta). \quad (5)$$

As a result, the solution of Eqn (1) has the form

$$\psi = \arctan\frac{x_3 + [x_3^2 + 4x_1(1-x_2)]^{0.5}}{2-2x_2}. \quad (6)$$

Having determined the 'key' angle ψ, we will find the rest of the parameters

$$\theta_{in} = 180^\circ - \beta - \psi, \quad (7)$$

$$\theta_{out} = \arcsin(n_\psi \sin\theta), \quad (8)$$

$$n_\psi = \frac{n_o n_e}{[n_o^2 \sin^2(v-\beta-\psi) + n_e^2 \cos^2(v-\beta-\psi)]^{0.5}}, \quad (9)$$

where n_ψ is the refractive index determining the phase velocity of the reflected e-wave in the direction of the vector $\boldsymbol{K}_{e2}$.

By varying the angles α, β, and v, we should take into account that the TIR of e-waves can present on the BC face. The corresponding critical angle θ_{TIR} depends on the inclination angle v of the optical axis and can be calculated from the expression similar to (6), but with other constants obtained from the Snell equation for critical TIR on the BC face:

$$\theta_{TIR} = \arctan\frac{z_3 + [z_3^2 + 4z_1(1-z_2)]^{0.5}}{2-2z_2}, \quad (10)$$

where

$$z_1 = \frac{1}{n_e^2}\sin^2 v + \frac{1}{n_o^2}\cos^2 v; \quad (11)$$

$$z_2 = \frac{1}{n_o^2}\sin^2 v + \frac{1}{n_e^2}\cos^2 v; \quad (12)$$

$$z_3 = \left(\frac{1}{n_e^2} - \frac{1}{n_o^2}\right)\sin 2v. \quad (13)$$

Expressions (2)–(13) allow one, for the known dispersions and temperature derivatives of the refractive indices, to calculate polarisation prisms made of any crystals, including biaxial ones, for any wavelengths and temperatures. However, in the case of biaxial crystals, these expressions are valid only for the waves propagating in the principal planes of the triaxial ellipsoid of refractive indices. In this case, it is necessary to use instead of n_o and n_e the pairs of refractive indices corresponding to the semiaxes of ellipses in the principal sections of the ellipsoid, and any of the axes of the chosen ellipse can play the role of the optical axis.

For the propagation of the e-ray indicated in Fig. 1, the angles α and v have the values $\alpha = \beta = 90^\circ$ and $v = 135^\circ$ for a prism made of a negative crystal and $\alpha = \beta = 90^\circ$, $v = 45^\circ$ for a prism made of a positive crystal. To calculate the linear dimensions of the prisms, it is necessary to know the angles δ_{1dr} of energy drifts of the e-waves (before reflection) and γ (after reflection). Note that, unlike δ_{1dr}, the letter γ denotes the angle of energy drift of the e-wave with respect to the long face of the prism, and this angle is not equal to the real angle δ_{2dr} of energy drift with respect to the wave vector $\boldsymbol{K}_{e2}$ of the e-wave after reflection. The procedure of calculation of these angles is as follows. Let δ_r be the angle between the ray Poynting vector $\boldsymbol{R}_e$ and the optical axis. Then, this angle is related by the classical expression to the angle δ_w formed by the wave vector $\boldsymbol{K}_e$ and the same optical axis:

$$\frac{\tan\delta_r}{\tan\delta_w} = \left(\frac{n_o}{n_e}\right)^2. \qquad (14)$$

It follows from (14) that the e-ray ($\boldsymbol{R}_e$) in negative crystals ($n_o > n_e$) makes an acute angle with the optical axis, which is always greater than the angle between this axis and the wave vector $\boldsymbol{K}_e$, and vice versa in positive crystals. We denote the acute angle between the vector $\boldsymbol{K}_{e1}$ and the optical axis in Fig. 2 by δ_{1w}. If $v > 90^\circ$ (negative crystals), then $\delta_{1w} = 180^\circ - (v - \beta + \alpha)$, and if $v < 90^\circ$ (positive crystals), then $\delta_{1w} = v - \beta + \alpha$. The angle δ_{1r} calculated from (14) allows us to find the modulus of the angle of the first energy drift of the e-wave at its input to an anisotropic prism: $\delta_{1dr} = |\delta_{1r} - \delta_{1w}|$. After reflection of the e-wave [when the angle ψ is already found from (6)], the angle δ_{2w} is determined from the geometry of Fig. 2, then the angle δ_{2r} is calculated from (14) and the angle γ is found again geometrically (or, if necessary, the angle $\delta_{2dr} = |\delta_{2r} - \delta_{2w}|$). In the case of the maximum filling of the prism volume by light, $\tan\delta_{1dr}$ and $\tan\gamma$ determine the prism dimensions.

Table 1, in which the notation corresponds to that in Fig. 1, presents the angular and linear characteristics calculated for prisms made of six optically inactive crystals most often used in polarisation optics, namely, $CaCO_3$, α-BaB_2O_4 (α-BBO), $LiIO_3$, $LiNbO_3$, YVO_4, and TiO_2. To demonstrate the influence of the wavelength dispersion, the calculations were performed for two wavelengths 1064 and 532 nm. Except the angular characteristics of the beam propagation, Table 1 gives the compression (anamorphism) coefficient d_e/d of a beam coming out to air and the ratio L/d of the prism length to its transverse size.

Because the angles δ_{1dr} and γ proved to be almost identical, the prism can be calculated by using only the angle δ_{1dr}. For the crystals pointed out above, the errors in the size of end faces and prism length are so small (no more than 2 %) that they can be compensated by the tolerances for linear dimensions.

The main disadvantage of such prisms is the great value of L/d, which restricts the maximum input diameter of a light beam by the value 0.5–1 mm for the real length of crystals $L = 10 - 20$ mm. For this reason, prisms are mainly used in fibre technologies, where collimated beams of diameter 0.3–0.5 mm are commonly used.

If the output BC face has no AR coating, optical losses K_r of the e-wave (Fresnel reflection losses) appear. These losses in an anisotropic crystal depend not only on the angle θ_{in} (θ_{out}) but also on the orientation angle v of the optical axis of the crystal. Optical losses calculated for the e-wave are presented in Table 1. Because the corresponding calculation procedure was not adequately described in the literature, we consider it in detail.

3. Reflection of the extraordinary wave

The Fresnel formulas for isotropic media are not valid for calculating K_r. In the most general case the propagation of light waves in any anisotropic crystals was studied in book [3]. However, the implicit vector expressions presented in this book are very difficult to use for applications. In no

Table 1. Angular and linear characteristics of a prism-parallelepiped polariser ($\alpha = \beta = 90^\circ$, see Figs 1 and 2).

Prism material (orientation angle of the optical axis)	λ/nm	n_o	n_e	δ_{1dr}/deg	γ/deg	θ_{out}/deg	d_e/d	L/d	K_r (%)
$CaCO_3$	1064	1.6425	1.4797	5.94	6.07	18.87	0.97	9.62	4.05
($v = 135^\circ$)	532	1.6629	1.4885	6.30	6.45	20.25	0.96	9.06	4.11
α-BBO	1064	1.6579	1.5203	4.94	5.01	15.90	0.98	11.57	4.61
($v = 135^\circ$)	532	1.6776	1.5359	5.03	5.11	16.38	0.97	11.36	4.80
$LiIO_3$	1064	1.8571	1.7165	4.49	4.55	16.27	0.97	12.73	7.19
($v = 135^\circ$)	532	1.8982	1.7480	4.70	4.77	17.41	0.97	12.16	7.57
$LiNbO_3$	1064	2.2340	2.1544	2.08	2.08	9.16	0.99	27.57	13.64
($v = 135^\circ$)	532	2.3248	2.2317	2.34	2.35	10.72	0.99	24.48	14.17
YVO_4	1064	1.9571	2.1650	5.75	5.86	24.41	0.93	9.94	9.76
($v = 45^\circ$)	532	2.0177	2.2508	6.21	6.36	27.57	0.91	9.18	10.06
TiO_2	1064	2.4793	2.7418	5.73	5.84	31.45	0.87	9.97	15.00
($v = 45^\circ$)	532	2.6678	2.9789	6.27	6.42	38.14	0.81	9.10	15.02

way pretending to novelty, we performed the standard study of the propagation of an electromagnetic wave through the interface of two media and considered separately the propagation of the e-wave in the plane containing the optical axis in a uniaxial crystal, which is often encountered in practice. As a result, we obtained the explicit and easily programmable expressions for calculating the reflection coefficient K_r of the extraordinary wave, which take into account the noncollinearity of the electric field and electric induction vectors and, correspondingly, the noncollinearity of the wave and ray vectors. The results of calculations of the energy reflection coefficients by these expressions coincide with the results presented in [3]. In addition, special measurements of the Brewster angles performed for $CaCO_3$ plates with different orientations of the optical axis showed that our formulas allow us to calculate accurately these angles.

Thus, the energy coefficient K_r of reflection of the e-wave from the end BC surface of the prism (Fig. 2) made of a uniaxial crystal so that its optical axis is parallel to the plane of incidence-refraction of this wave is calculated from the expression

$$K_r = \left[\frac{1-(A+B\tan^2\theta_{is})^{0.5}}{1+(A+B\tan^2\theta_{is})^{0.5}}\right]^2, \tag{15}$$

where

$$A = \left(\frac{n_{is}}{n_v}\right)^2; \tag{16}$$

$$B = A - \left(\frac{n_{is}}{n_o}\right)^2\left(\frac{n_{is}}{n_e}\right)^2; \tag{17}$$

$$n_v = \frac{n_o n_e}{(n_0^2\sin^2 v + n_e^2\cos^2 v)^{0.5}}; \tag{18}$$

n_{is} is the refractive index of the isotropic medium (it is assumed that $n_{is}=1$ in air); θ_{is} is the angle between the normal N_{BC} and vector $\boldsymbol{K}_{e3}$ in the isotropic medium (in our case, $\theta_{is}=\theta_{out}$).

From the condition $K_r=0$, the expression can be easily obtained for the two possible Brewster angles θ_{out}^{Br} corresponding to the two mirror (with respect to the normal N_{BC}) orientations of the wave vector $\boldsymbol{K}_{e3}$ in the isotropic medium:

$$\tan\theta_{out}^{Br} = \pm\left(\frac{1-A}{B}\right)^{0.5}. \tag{19}$$

It is obvious that the moduli of both possible angles θ_{out}^{Br} in the isotropic medium are identical (as should be according to the Snell reflection law). However, the corresponding Brewster angles θ_{in}^{Br} for the extraordinary wave differ not only by signs but also by magnitudes. The expression for these angles can be easily obtained from the Snell refraction law on the BC face:

$$\tan\theta_{in}^{Br} = \left[0.5n_v^2\left(\frac{1}{n_e^2}-\frac{1}{n_o^2}\right)\sin 2v + \frac{n_v^2}{\tan\theta_{out}^{Br}}\right]^{-1}. \tag{20}$$

The function $\tan\theta_{out}^{Br}$ in (20) is taken from (19) with the appropriate sign, which determines the value of the possible angle θ_{in}^{Br}.

Upon passage to the limit of isotropic media, when $n_o=n_e=n$, expressions (15), (19), and (20) transform to the usual Fresnel and Brewster formulas.

4. Prism with minimised reflection losses

Having determined the Brewster angles for the e-waves, we construct a prism in which the p-polarised e-wave reflected from the AB face comes outside through the BC face without reflection losses. This is achieved by decreasing the inclination angle β of the AB face (see Fig. 2) down to the value determined by the given condition. Figure 3 shows the section of such a prism, and Table 2 presents the angular and linear characteristics calculated at wavelengths 1064 and 532 nm for polarisation beamsplitters made of six crystals mentioned above. The angles δ_{1dr} и γ differ now so strongly (the scale in Fig. 3 is distorted for clearness) that the input and output faces of the prism have substantially different dimensions. The ratio L/d is the same as in Fig. 1.

To demonstrate the influence of the dispersion of the refraction indices on the deviation angle θ_{out} of the e-beam, we present in Table 2 the values of this angle and corresponding reflection coefficient for the alternative wavelength (for a prism calculated for the wavelength 1064 nm, the alternative wavelength is 532 nm, and vice versa). One can easily see that the moduli of the difference $|\theta_{out}^{alt}-\theta_{out}^{Br}|$ change in the range $1.4^\circ-15^\circ$. They are especially large in prisms made of $LiNbO_3$, YVO_4, and TiO_2 crystals. This dispersion can be used for spatial splitting of beams with optical frequencies obtained upon cascade frequency doubling by means of various nonlinear crystals, including periodically poled crystals. In this respect, of interest is a TiO_2 rutile prism. If this prism is made so that the p-polarised 1064-nm radiation comes out from the BC face at the Brewster angle, then the second harmonic radiation with the same polarisation (obtained, for example, in periodically poled $LiNbO_3$ or KTP crystals) will experience TIR from this face at an angle exceeding the critical angle by more than 1°. This radiation can be coupled outside normally to the DC face if the latter is appropriately 'inclined'.

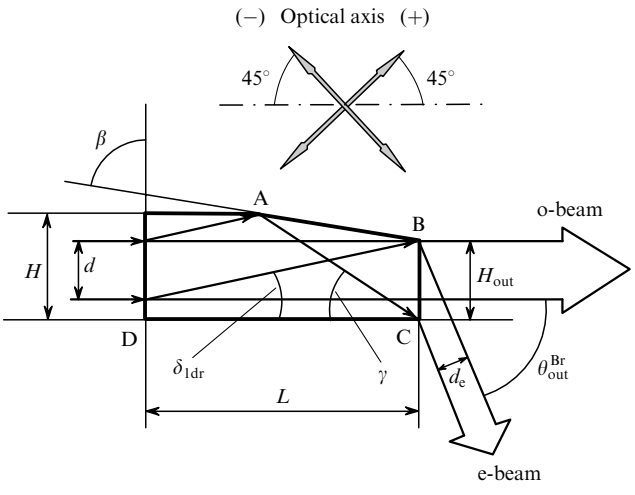

Figure 3. Propagation of beams in a prism with the Brewster output of the e-wave (the figure scale is distorted for clearness).

Table 2. Angular and linear characteristics of a polarisation beamsplitter with the Brewster output of the extraordinary beam (see Figs 2 and 3).

Prism material (orientation angle of the optical axis)	λ/nm	β/deg	γ/deg	θ_{in}^{Br}/deg	θ_{out}^{Br}/deg	d_e/d	H/d	H_{out}/d	θ_{out}^{alt}/deg	K_r^{alt} (%)
$CaCO_3$	1064	79.46	27.92	30.99	57.15	0.64	1.83	1.19	59.79	0.09
($v = 135°$)	532	79.96	27.33	30.68	57.37	0.64	1.80	1.18	54.90	0.06
α-BBO	1064	78.68	28.30	30.84	57.68	0.63	1.88	1.18	59.16	0.02
($v = 135°$)	532	78.92	27.92	30.55	57.96	0.62	1.87	1.18	56.54	0.02
$LiIO_3$	1064	79.74	25.55	28.22	60.67	0.56	1.84	1.15	64.27	0.23
($v = 135°$)	532	80.21	25.85	27.72	61.16	0.55	1.82	1.14	57.92	0.13
$LiNbO_3$	1064	79.76	22.74	24.16	65.49	0.46	1.93	1.10	74.37	3.71
($v = 135°$)	532	80.42	21.68	23.33	66.29	0.44	1.90	1.09	59.76	0.84
YVO_4	1064	82.74	20.84	24.87	64.00	0.49	1.67	1.11	74.13	4.48
($v = 45°$)	532	83.62	19.56	24.08	64.76	0.47	1.61	1.10	57.44	0.91
TiO_2	1064	85.23	15.64	20.30	68.95	0.38	1.52	1.07	TIR	100
($v = 45°$)	532	86.53	13.57	18.89	70.40	0.36	1.42	1.06	55.46	4.7

5. Dispersion-free thermally stable polarisation beamsplitter

The example of a prism with the Brewster output coupler for the e-beam shows that, by varying the tilt of the AB face, we can produce polarisation beamsplitters almost with any splitting angle for polarised beams. For example, if the inclination angle β of the AB face is taken to be 45° and the optical axis is oriented strictly at the angle $v = 135°$ (for negative crystals) or 45° (for positive crystals), we obtain a prism in which the e-beam comes outside not through the BC face but through the DC face at an angle of 90° to the o-beam (Fig. 4). An important feature of such a prism is the independence of this angle of temperature T, the wavelength of light λ and even on a crystal (i.e., of the values of n_o and n_e). Analysis of expressions (1)–(9) shows that the angle of reflection of the e-wave incident on the AB face at an angle of 45° is also equal to 45° for any λ, T, n_o, and n_e. Note that this is valid only for the two orientations of the optical axis pointed out above. The mechanical (thermal) distortion of the prism form, which could change the angles of reflection and incidence, is absent here. The reason is that for the orientation angles of the axis of a uniaxial crystal equal to ±45°, the contributions from two different expansion coefficients to the change in the lengths of edges of a base parallelepiped prove to be the same, while the AB face inclined at an angle of 45° moves parallel to itself during the temperature variation of the prism dimensions. The only characteristic that changes with changing temperature and wavelength is the displacement L_{dr} of the e-beam on the output DC face. However, the absolute variations ΔL_{dr} are negligible, because for angles $\gamma \simeq \delta_{1dr} \approx 6°$ and the beam diameter ~1 mm, the values of L_{dr} are so small (~0.1 mm) that ΔL_{dr} can be neglected.

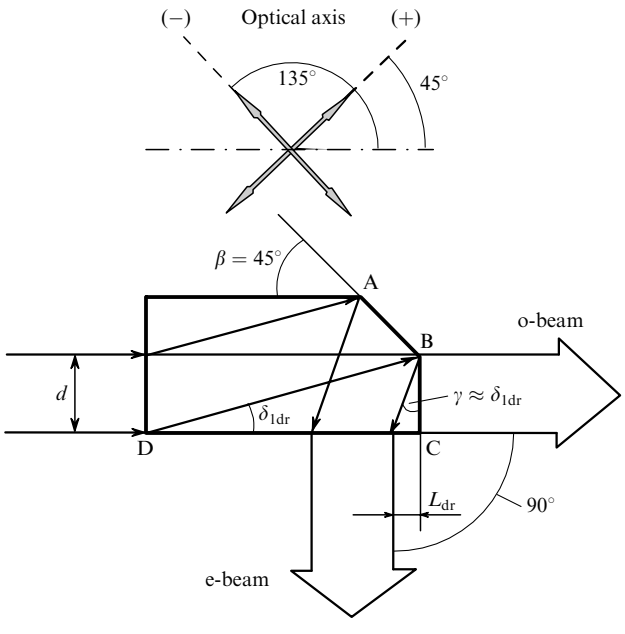

Figure 4. Propagation of beams in a prism with the 90° deviation of the e-beam (the figure scale is distorted for clearness).

6. Combined polarisation beamsplitters

Prisms described above can be used in combinations of the type shown in Fig. 5. Because the e-wave experiences an even number of reflections, such combined polarisation beamsplitters are devoid of the temperature and dispersion dependences of the angular position of the e-beam. Prism 2 in the scheme in Fig. 5b also corrects the astigmatic distortion of the beam cross section, while astigmatism is absent at all in the scheme in Fig. 5a. By varying the gap S between prisms, we can obtain virtually any distances between the output parallel beams with prisms of a small size. Such polarisation beamsplitters can find applications, for example, in optical circulators (isolators) used at high radiation powers. Such beamsplitters in polarisation-independent isolators allow one to place a Faraday rotator in each beam, where the light beam will propagate strictly along the axis of the active element (rather than with displacement, as in isolators with one common Faraday element), filling completely its aperture. This will improve the homogeneity of the magnetic-field distribution over the beam cross section and reduce the radiation power density in the element, thereby improving the isolator parameters (losses, isolation, radiation resistance).

Note that in simpler cases, when there is no need to split spatially the forward and backward beams with orthogonal polarisations, prisms 2 in combined beamsplitters (Fig. 5)

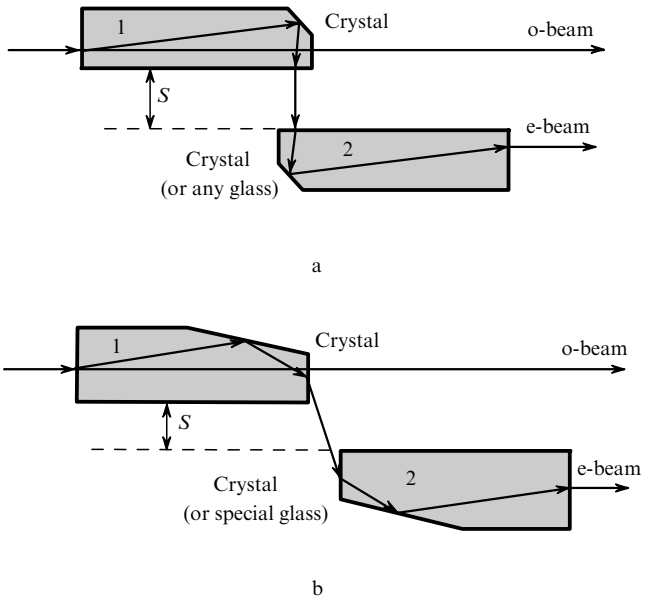

Figure 5. Combined polarisation beamsplitters devoid of the dispersion and temperature dependences of the angular position of beams (symmetric propagation of beams corresponds only to crystal prisms): combinations of prisms with the 45° TIR face (a) and the Brewster refraction of the e-beams (b); 1 and 2: prisms.

can be made of glass. The scheme in Fig. 5a admits the use of any glass, while in the scheme in Fig. 5b the astigmatism of the e-beam should be completely compensated by using a glass with the refractive index $n = d/d_e$ (see Table 2). Because the Brewster angle of incidence of a beam on the input face of a glass prism will differ from the external Brewster angle in a crystal prism, the second prism should be appropriately inclined with respect to the first prism. In addition, if the parallelism of the output beams is preserved, the angle β in a glass prism also should be changed. All these calculations follow obviously from the propagation geometry of the beams, and therefore we do not present them here.

7. Experimental tests

We tested the prisms described above by measuring the calculated deviation angles for the e-beams at wavelengths of 1064 and 532 nm and verifying the thermal stability and radiation resistance of the 90° prism. Two prisms with the 1-mm apertures (Figs 1 and 4) made of the high-quality calcite (Unikum) were studied. The optical axes were oriented in these prisms with an accuracy of $\pm 15'$, the prism angles were made with an error of $\pm 5'$, and the working faces were polished with optical quality and had no AR coatings.

A pulsed semiconductor laser was used as a radiation source. The laser radiation was amplified in two amplifiers based on an isotropic single-mode Yb^{3+}-doped silica fibre. To avoid SRS effects, we used a special fibre with an increased mode diameter ($\sim$14 μm) in the second amplifier. The laser emitted 2.1-kW, 5-ns pulses at a wavelength of 1064 nm with a pulse repetition rate of 50 kHz and a laser linewidth of 0.2 nm. The laser beam was emitted in the form of a collimated Gaussian beam of diameter 0.4 mm with a predominantly vertical polarisation (which was produced with a fibre polarisation controller). The beam was collimated with a graded index (GRIN) lens [4]. A specific feature of this lens is that it can be easily made a short-focus lens without spherical aberration, and the focal point can be located near the flat input end of the lens at any small distance from it. It is very convenient because allows the incorporation of the lens with a single-mode fibre into a single rigid collimator unit. As a result, the pulsed power density in the near-field zone achieved $\sim$1.7 MW cm^{-2}.

This beam polarised along the Z axis was directed along the X axis on a periodically poled KTP crystal where it was partially (7 %) converted to the second harmonic with the same polarisation. Behind the crystal, a half-wave plate was located whose optical axis made an angle of 22.5° with the polarisation plane of the input beam and the normal to the prism base. The plate operating at a wavelength of 1064 nm rotated the polarisation plane of radiation at this wavelength by 45° and transformed polarisation of the green light to elliptic polarisation. The beam transformed in this way was directed on the prism under study where it was split into the o- and e-waves. The IR radiation was detected with a night vision device.

The deviation angles of the e-beams were measured trigonometrically by means of a screen placed at a distance of 1000 ± 5 mm from the prism. The distance between the centres of the beams on the screen measured with an error of ± 1 mm, so that the angular measurement error was $\pm 15'$. Within this measurement error, the output angles θ_{out} of the e-beam measured at the two wavelengths coincided perfectly with the angles calculated for calcite (Table 1).

To control the temperature stability of the 90° output angle of the e-beam in the prism (Fig. 4), the prism was heated in a sealed cylindrical invar heater with quarts windows. The error of measurement of the relative variations in the output angles of the e-beam was smaller than the measurement error of the angles themselves, being $\pm 2'$ according to our estimate. Within this experimental error, no changes were observed depending on the wavelength in the temperature range from room temperature to 70 °C.

A 90° prism placed inside a sealed heater (to protect from dust) was tested for the radiation resistance at $\lambda = 1064$ μm. In front of the prism, a quartz lens with the focal length $F = 30$ mm was mounted to focus the Gaussian laser beam into a waist of diameter $\sim$100 μm, in which the radiation power density was $\sim$27 MW cm^{-2}. The prism under study was located at three different distances from this focus, in particular, so that the waist centre was located on the 45° TIR face. In each position, the prism was irradiated for 30 min. No damage of the working faces of prisms was found.

8. Conclusions

Based on the exact solutions of the Snell equation for the TIR of the e-wave and modified expressions for the Brewster refraction of this wave, we have developed simple and small polarisation prisms for applications with small-diameter laser beams.

The expressions convenient for programming obtained in the paper and the data presented in Tables 1 and 2 allow any experimenter in optics (not necessarily well familiar with crystal optics) to design polarisation beamsplitters (polarisers) of this class.

The main disadvantage of the prisms, which restricts their application, is a small diameter of light beams. A more

detailed analysis of some features of TIR of the e-waves showed that this disadvantage can be eliminated because it is possible to fabricate compact monoprisms with the splitting angles of polarised beams achieving tens of degrees and 'zero' reflection losses, which can be used for operating with beams of greater diameters (up to 10 mm and more). The results of this analysis will be published elsewhere.

References

1. Stroganov V.I., Samarin V.I. *Kristallografia*, **3**, 652 (1975).
2. Stroganov V.I., Muryi A.A. *Opt. Zh.*, **70** (11), 76 (2003).
3. Fedorov F.I. *Optika anizotropnykh sred* (Optics of Anisotropic Media) (Moscow: URSS, 2004).
4. Mikaelyan A.L. *Opticheskie metody v informatike* (Optical Methods in Informatics) (Moscow: Nauka, 1990).